Combust. Sci. Technol., 185: 226–248, 2013

ISSN: 0010-2202 print/1563-521X online
DOI: 10.1080/00102202.2012.715607

Taylor & Francis
Taylor & Francis Group

OUTWARDLY PROPAGATING SPHERICAL FLAMES WITH THERMALLY SENSITIVE INTERMEDIATE KINETICS AND RADIATIVE LOSS

Huangwei Zhang,[1] Peng Guo,[1] and Zheng Chen[1,2]
[1]*State Key Laboratory for Turbulence and Complex Systems, Department of Mechanics and Aerospace Engineering, College of Engineering, Peking University, Beijing, China*
[2]*Department of Aeronautics and Astronautics, College of Engineering, Peking University, Beijing, China*

The outwardly propagating spherical flames with thermally sensitive intermediate kinetics and radiative loss are analyzed within the framework of large activation energy and quasi-planar assumptions. The relationship between the flame propagation speed and flame radius are derived in theoretical analysis. Based on this relationship, the spherical flame propagation and extinction are analyzed. The flame propagation speed and extinction limit are shown to be strongly affected by fuel and radical Lewis numbers and radiative loss. It is demonstrated that the spherical flame propagation is always enhanced by the increase of the radical Lewis number, and that the flame propagation speed correlates well with the peak radical concentration. The radiative loss is shown to affect quantitatively but not qualitatively the dependence of the Markstein length on the fuel and radical Lewis numbers. Moreover, it is found that the flammable region of positively stretched spherical flame can be extended by decreasing the fuel Lewis number or increasing the radical Lewis number, and that the self-extinguishing flame can be observed for mixtures with small fuel Lewis number andlor large radical Lewis number. The linear and quartic heat loss models are compared, and these two models are found to have qualitatively and even quantitatively similar influence on spherical flame propagation when the heat loss intensities are properly specified. Furthermore, transient numerical simulations of spherical flame propagation at finite reaction rate are conducted to demonstrate the validity of theoretical results.

Keywords: Extinction limit; Lewis number; Propagating spherical flame; Radiative loss; Two-step chemistry

INTRODUCTION

Due to the simple one-dimensional configuration, the propagating spherical flame has been extensively investigated by asymptotic analysis in the literature

Received 7 April 2012; revised 21 June 2012; accepted 23 July 2012.

The current affiliation for Huangwei Zhang is Department of Engineering, University of Cambridge, Cambridge, UK.

Address correspondence to Zheng Chen, State Key Laboratory for Turbulence and Complex Systems (SKLTCS), Department of Mechanics and Aerospace Engineering, Department of Aeronautics and Astronautics, College of Engineering, Peking University, Beijing 100871, China. E-mail: cz@pku.edu.cn

(Bechtold et al., 2005; Bechtold and Matalon, 1987; Buckmaster and Lee, 1992; Champion et al., 1986; Chen et al., 2010; Chen and Ju, 2007; Chung and Law, 1988; Frankel and Sivashinsky, 1983, 1984; He, 2000; Kelley et al., 2012; Ronney and Sivashinsky, 1989). However, the one-step, irreversible, global reaction model was employed in all these studies, and the fuel is directly converted into products and heat. As a result, the role of energetic active radicals is not considered. In practical combustion of hydrocarbon fuels, numerous elementary reactions related to fuel and reactive intermediate species appear (Law, 2006; Westbrook, 2000). Therefore, spherical flame propagation is affected not only by the properties of fuel, but also by those of intermediate species (especially radicals involved in chain branching reactions).

In our recent studies (Zhang and Chen, 2011; Zhang et al., 2013), the adiabatic spherical flame propagation with thermally sensitive intermediate kinetics was studied based on the following simplified form of the Zel'dovich–Liñán model (Linan and Williams, 1993; Zeldovich et al., 1985) proposed by Dold and coworkers (Dold, 2007; Dold et al., 2002, 2003, 2004):

$$F + Z \rightarrow 2Z : k_B = A_B \exp(-T_B/T) \tag{1a}$$

$$Z + M \rightarrow P + M : k_C = A_C \tag{1b}$$

where *F, Z, P*, and *M* represent fuel, radical, product, and the third body, respectively. A_B and T_B are the frequency factor and activation temperature of reaction (1a), respectively, while A_C is the frequency factor of reaction (1b). The above model involves a thermally sensitive chain branching reaction (1a) with a rate constant k_B in Arrhenius form and a completion reaction (1b) with a rate constant k_C, which is equal to the frequency factor A_C and is independent of temperature T. Besides propagating spherical flames, flame balls and propagating planar flames were also investigated based on the above model (Dold, 2007; Dold et al., 2002, 2003, 2004; Gubernov et al., 2008a, 2008b, 2011; Sharpe and Falle, 2011).

However, the radiative loss was not included in the work by Zhang and Chen (2011). It is well known that radiative heat transfer is a dominant mechanism for near limit flames (Ju et al., 2001). According to the theory based on one-step chemistry (Bechtold et al., 2005; Chen and Ju, 2007; Ronney and Sivashinsky, 1989), the interaction of flame stretch and radiative loss greatly affects the spherical flame propagation and extinction. However, spherical flame propagation with thermally sensitive intermediate kinetics and radiative loss was not studied previously. As a result, how the radical affects the spherical flame propagation and extinction remains unknown. The first objective of this study is therefore to reveal the effects of fuel and radical Lewis numbers and radiation on spherical propagation and extinction.

The outwardly propagating spherical flame method is currently one of the most favorable methods for measuring the laminar flame speed and Markstein length (see Chen, 2011, and references cited therein). Radiation transfer is inevitable in practical combustion experiments, and the effect of radiation on flame speed measurements has been investigated in previous studies (Buckmaster and Lee, 1992; Chen, 2010; Chen et al., 2007, 2010; Matalon and Bechtold, 2009; Taylor, 1991). According to the theory based on one-step chemistry (Chen et al., 2010; Matalon and Bechtold,

2009), the Markstein length strongly depends on the fuel Lewis number and heat loss intensity. However, it is still not clear how the combined effects of radical Lewis number and radiative loss affect the Markstein length. Therefore, the second objective of this study is to assess the effects of fuel and radical Lewis numbers and radiation on the Markstein length.

Based on the objectives discussed above, the outwardly propagating spherical flames with thermally sensitive intermediate kinetics and radiative loss are analyzed in the following. First, the mathematical model is presented and theoretical analysis is conducted. Then, based on the theoretical results, the effects of fuel and radical Lewis numbers and radiation on spherical flame propagation and extinction and the Markstein length are investigated. Moreover, transient numerical simulations are conducted to validate the theoretical results. Finally, the conclusions are presented.

MATHEMATICAL MODEL

Outwardly propagating spherical flames with thermally sensitive intermediate kinetics and radiative loss are studied here using the classical reactive-diffusive model (Clavin, 1985; Joulin and Clavin, 1979). By using the same nondimensionalization procedure employed by Zhang and Chen (2011), we have the following nondimensional equations in a spherical coordinate for fuel mass fraction Y_F, radical mass fraction Y_Z, and temperature T:

$$\frac{\partial Y_F}{\partial t} = \frac{1}{Le_F}\frac{1}{r^2}\frac{\partial}{\partial r}\left(r^2\frac{\partial Y_F}{\partial r}\right) - \omega \tag{2a}$$

$$\frac{\partial Y_Z}{\partial t} = \frac{1}{Le_Z}\frac{1}{r^2}\frac{\partial}{\partial r}\left(r^2\frac{\partial Y_Z}{\partial r}\right) + \omega - Y_Z \tag{2b}$$

$$\frac{\partial T}{\partial t} = \frac{1}{r^2}\frac{\partial}{\partial r}\left(r^2\frac{\partial T}{\partial r}\right) + QY_Z - H \tag{2c}$$

in which the variables t and r are temporal and spatial coordinates, respectively. Le_F and Le_Z are the Lewis numbers of fuel and radical species, respectively. Q represents the specific heat release of the completion reaction (1b). ω is the nondimensional reaction rate in the following form (Dold et al., 2003; Zhang and Chen, 2011):

$$\omega = \beta^2 Y_F Y_Z \exp\left[\beta\frac{T-1}{1+\sigma(T-1)}\right] \tag{3}$$

with β being the Zel'dovich number and σ the temperature ratio defined by Dold et al. (2003) and Zhang and Chen (2011). Due to the constant density assumption in the reactive-diffusive model, there are no convective fluxes in the governing equations [Eqs. (2a)–(2c)].

Unlike our previous study (Zhang and Chen, 2011), we consider in the energy equation [Eq. (2c)] the nondimensional volumetric heat loss in the form of $H = h[(T+\gamma)^n - \gamma^n]$ (in the dimensional form it is $\tilde{H} = \tilde{h}(\tilde{T}^n - \tilde{T}_\infty^n)$), in which h

denotes the heat loss intensity and $\gamma = 1/\sigma - 1$ (Zhang and Chen, 2011). The quantity γ is assumed to be 0.286 in both theoretical analysis and numerical validations of the present study, according to typical initial conditions and characteristics of hydrocarbon fuels (Dold et al., 2003). The parameter n determines the type of the heat loss: $n = 4$ for radiative heat loss from an optically thin medium, and $n = 1$ for a phenomenological heat loss that depends linearly on temperature. In previous studies (Chen et al., 2010; Chen and Ju, 2007; Dold, 2007; Dold et al., 2002, 2003, 2004), only linear heat loss (i.e., $n = 1$) was considered. In this study, both the linear and quartic heat losses are considered by specifying $n = 1$ and $n = 4$, respectively. Comparison between the effects of these two types of heat loss on spherical flame propagation is conducted in the section entitled "Comparison Between Linear and Quartic Heat Loss Models."

In a coordinate ($\tau = t$, $\xi = r - R(t)$) attached to the propagating flame front, $R = R(t)$, the nondimensional governing equations take the following form:

$$\frac{\partial Y_F}{\partial \tau} - U\frac{\partial Y_F}{\partial \xi} = \frac{1}{Le_F}\frac{1}{(\xi + R)^2}\frac{\partial}{\partial \xi}\left[(\xi + R)^2\frac{\partial Y_F}{\partial \xi}\right] - \omega \tag{4a}$$

$$\frac{\partial Y_Z}{\partial \tau} - U\frac{\partial Y_Z}{\partial \xi} = \frac{1}{Le_Z}\frac{1}{(\xi + R)^2}\frac{\partial}{\partial \xi}\left[(\xi + R)^2\frac{\partial Y_Z}{\partial \xi}\right] + \omega - Y_Z \tag{4b}$$

$$\frac{\partial T}{\partial \tau} - U\frac{\partial T}{\partial \xi} = \frac{1}{(\xi + R)^2}\frac{\partial}{\partial \xi}\left[(\xi + R)^2\frac{\partial T}{\partial \xi}\right] + QY_Z - h[(T + \gamma)^n - \gamma^n] \tag{4c}$$

in which $U = \mathrm{d}R(t)/\mathrm{d}t$ is the flame propagation speed.

In this study, we assume that the reactive-diffusive structure of the propagating spherical flame is quasiplanar ($R >> 1$, $\xi \sim \mathrm{O}(1)$) (Chen et al., 2010; Frankel and Sivashinsky, 1983, 1984), and that the flame propagation is in a quasisteady state ($\partial/\partial\tau = 0$) in the coordinate moving with the flame front. This quasisteady assumption has been widely used in previous studies (Chen et al., 2010; Chen and Ju, 2007; Frankel and Sivashinsky, 1983, 1984), and it is validated by transient numerical simulations in the "Numerical Validation" section of this article. Moreover, in the limit of large activation energy, chemical reactions occur within the infinitesimally thin flame sheet ($r = R(t)$), and outside of the flame sheet, the flow can be considered to be chemically frozen (i.e., $\omega = 0$) (Dold, 2007; Dold et al., 2002, 2003, 2004). Based on these assumptions and simplifications, Eqs. (4a)–(4c) can be reduced to

$$\frac{d^2 Y_F}{d\xi^2} + \left(ULe_F + \frac{2}{R}\right)\frac{dY_F}{d\xi} = 0 \tag{5a}$$

$$\frac{d^2 Y_Z}{d\xi^2} + \left(ULe_Z + \frac{2}{R}\right)\frac{dY_Z}{d\xi} - Le_Z Y_Z = 0 \tag{5b}$$

$$\frac{d^2 T}{d\xi^2} + \left(U + \frac{2}{R}\right)\frac{dT}{d\xi} + QY_Z - h[(T + \gamma)^n - \gamma^n] = 0 \tag{5c}$$

According to the asymptotic analysis conducted by Dold and coworkers (Dold, 2007; Dold et al., 2003), the following conditions must hold across or at the flame front ($\xi = 0$):

$$[Y_F] = [Y_Z] = [T] = \left[\frac{dT}{d\xi}\right] = \left[\frac{1}{Le_F}\frac{dY_F}{d\xi} + \frac{1}{Le_Z}\frac{dY_Z}{d\xi}\right] = T - 1 = Y_F\frac{dT}{d\xi} = 0 \quad (6)$$

where the square brackets represent the difference between the quantities on the unburned and burned sides, i.e., $[f] = f(\xi = 0^+) - f(\xi = 0^-)$.

We only consider the fuel-lean case in this study. Therefore, the nondimensional boundary conditions for Y_F, Y_Z, and T are as follows:

$$\xi = +\infty, \qquad Y_F = 1, \qquad Y_Z = 0, \; T = 0 \quad (7a)$$

$$\xi = -\infty, \qquad dY_F/d\xi = 0, \qquad dY_Z/d\xi = 0, \qquad dT/d\xi = 0 \quad (7b)$$

THEORETICAL ANALYSIS

The governing equations [Eqs. (5a)–(5c)] with conditions at the flame front [Eq. (6)] and boundary conditions [Eqs. (7a) and (7b)] can be solved analytically in the burned ($\xi \le 0$) and unburned ($\xi \ge 0$) regions, respectively. The analytical solution for the fuel mass fraction is

$$Y_F(\xi) = \begin{cases} 0 & for \quad \xi \le 0 \\ 1 - \exp[-(ULe_F + 2/R)\xi] & for \quad \xi \ge 0 \end{cases} \quad (8)$$

and that for the radical mass fraction is

$$Y_Z(\xi) = \begin{cases} Y_{Zf}\exp(\theta_1\xi) & for \quad \xi \le 0 \\ Y_{Zf}\exp(\theta_2\xi) & for \quad \xi \ge 0 \end{cases} \quad (9)$$

with

$$\theta_{1,2} = \frac{-(ULe_Z + 2/R) \pm \sqrt{(ULe_Z + 2/R)^2 + 4Le_Z}}{2} \quad (10)$$

In Eq. (9), Y_{Zf} is the radical mass fraction at the flame front ($\xi = 0$). According to the requirement of $[Le_F^{-1}dY_F/d\xi + Le_Z^{-1}dY_Z/d\xi] = 0$ at $\xi = 0$ in Eq. (6), we have

$$Y_{Zf} = \frac{Le_Z(U + 2/RLe_F)}{\sqrt{(ULe_Z + 2/R)^2 + 4Le_Z}} \quad (11)$$

The nondimensional heat loss intensity is usually much less than unity, i.e., $h << 1$ (Chen and Ju, 2008; Clavin, 1985; Ju et al., 2001; Zeldovich et al., 1985). Therefore, the temperature equation [Eq. (5c)] can be solved in an asymptotic manner. By neglecting the second and higher order terms of $O(h^2)$, we obtain the

following asymptotic expressions for the temperature distributions in the burned and unburned regions:

$$T(\xi) = T_0(\xi) + hT_1(\xi) \quad for\ \xi \le 0 \quad \text{and}\ \xi \ge 0 \tag{12}$$

with

$$T_0(\xi) = \begin{cases} 1 + \frac{QY_{Zf}}{\theta_1^2 + \left(U + \frac{2}{R}\right)\theta_1} - \frac{QY_{Zf}}{\theta_1^2 + \left(U + \frac{2}{R}\right)\theta_1} e^{\theta_1 \xi} & for \quad \xi \le 0 \\ \left[1 + \frac{QY_{Zf}}{\theta_2^2 + \left(U + \frac{2}{R}\right)\theta_2}\right] e^{-\left(U + \frac{2}{R}\right)\xi} - \frac{QY_{Zf}}{\theta_2^2 + \left(U + \frac{2}{R}\right)\theta_2} e^{\theta_2 \xi} & for \quad \xi \ge 0 \end{cases} \tag{13}$$

$$T_1(\xi) = \begin{cases} -\int_{\xi}^{\infty} \int_{-\infty}^{\eta} I(\varsigma) e^{\left(U + \frac{2}{R}\right)(\varsigma - \eta)} d\varsigma d\eta \\ \quad + \int_{0}^{\infty} \int_{-\infty}^{\eta} I(\varsigma) e^{\left(U + \frac{2}{R}\right)(\varsigma - \eta)} d\varsigma d\eta & for \quad \xi \le 0 \\ \int_{\xi}^{\infty} \int_{\eta}^{\infty} I(\varsigma) e^{\left(U + \frac{2}{R}\right)(\varsigma - \eta)} d\varsigma d\eta - \frac{\int_{\xi}^{\infty} e^{-\left(U + \frac{2}{R}\right)\eta} d\eta}{\int_{0}^{\infty} e^{-\left(U + \frac{2}{R}\right)\eta} d\eta} \\ \quad \int_{0}^{\infty} \int_{\eta}^{\infty} I(\varsigma) e^{\left(U + \frac{2}{R}\right)(\varsigma - \eta)} d\varsigma d\eta & for \quad \xi \ge 0 \end{cases} \tag{14}$$

where $I(\varsigma) = [T_0(\varsigma) + \gamma]^n - \gamma^n$.

Substituting the above temperature distribution into the requirement of heat flux continuity, $[dT/d\xi] = 0$ at $\xi = 0$, in Eq. (6), we obtain the following algebraic relationship between the flame propagation speed U and flame radius R:

$$\frac{QY_{Zf}}{\theta_1 + U + 2/R} - \frac{QY_{Zf}}{\theta_2} - (U + 2/R) = h(U + 2/R) \int_{0}^{\infty} \int_{-\infty}^{\eta} I(\varsigma) e^{(U + 2/R)(\varsigma - \eta)} d\varsigma d\eta \tag{15}$$

With the help of Eq. (15), we can investigate the effects of fuel and radical Lewis numbers and radiation on the propagation and extinction of outwardly propagating spherical flame [by changing Le_F, Le_Z, and h in Eq. (15)]. Since the influences of heat release on spherical flame propagation are not considered in this study, the normalized heat of reaction Q is fixed to be 2.0, a value that is representative for typical hydrocarbon combustible mixtures initially at 300 K (Dold et al., 2004).

It is noted that Eq. (15) is derived under the quasiplanar assumption ($R >> 1$). Therefore, Eq. (15) holds only for spherical flames with large flame radii. Adiabatic spherical flame propagation was analyzed in Zhang and Chen (2011) without employing the quasiplanar assumption. The result in Zhang and Chen (2011) is found to reduce to Eq. (15) in the limit of $R >> 1$ and $h = 0$, which demonstrates the consistency of the present analysis. The comparison is shown in Figure 1. As expected, the difference between the predication by the present theory and that by Zhang and Chen (2011) is shown to decrease with the flame radius. It is demonstrated that good agreement can be achieved for $R \ge 10$. Therefore, in the following

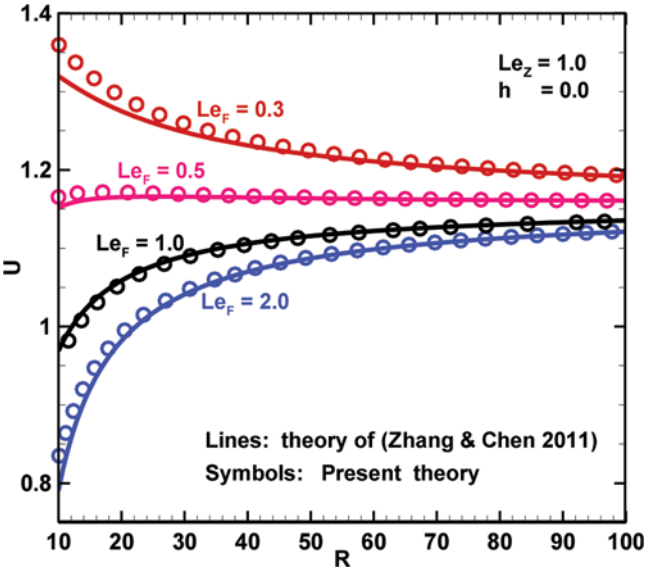

Figure 1 Spherical flame propagation speed as a function of flame radius. (Figure is provided in color online.)

section, the radiative spherical flame propagation with $R \geq 10$ is studied with the help of Eq. (15).

It can be readily proved that, in the limit of infinite flame radius ($R \to \infty$) and linear heat loss ($n = 1$), Eq. (15) reduces to previous result for non-adiabatic planar flames by Dold and coworkers (Dold, 2007; Dold et al., 2002, 2003, 2004). Therefore, the present analysis is consistent with that of Dold et al. (Dold, 2007; Dold et al., 2002, 2003, 2004) for planar flames with heat loss depending linearly on temperature. Moreover, for linear heat loss ($n = 1$), the exact temperature distribution can be solved from Eq. (5c). Comparison between exact solutions and asymptotic solutions for $n = 1$ shows good quantitative agreement. Therefore, it is reasonable to neglect the high order terms of $O(h^2)$ in the temperature distribution [Eq. (12)].

RESULTS AND DISCUSSION

In this section, the outwardly propagating spherical flames are studied using Eq. (15). In the first three subsections, the radiative heat loss (i.e., $H = h[(T+\gamma)^n - \gamma^n]$ with $n = 4$) is considered. In the last subsection, the linear ($n = 1$) and quartic ($n = 4$) heat loss models are compared.

Properties of Spherical Flame Propagation

The properties of spherical flame propagation are studied by solving Eq. (15) at different fuel and radical Lewis numbers and radiative loss intensities. Figure 2 shows the influence of radiative loss on spherical flame propagation. It is seen that there are two branches in the U–R diagram: the fast stable one and the slow unstable

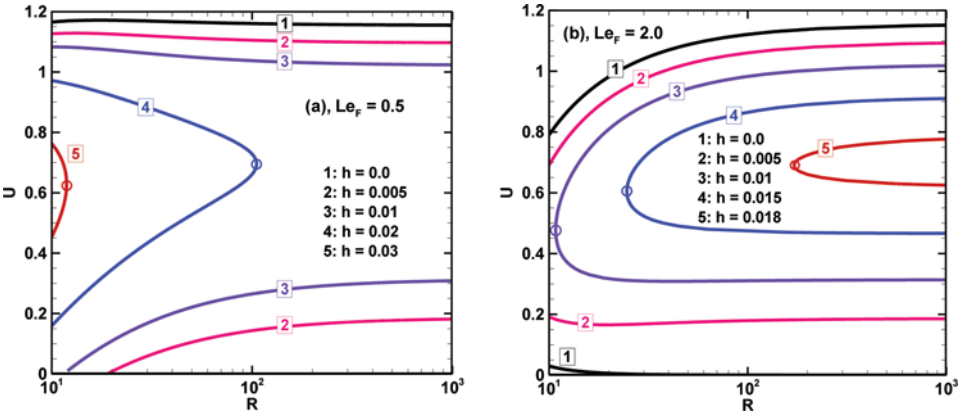

Figure 2 Spherical flame propagation at different radiative loss intensities. (Figure is provided in color online.)

one. Only the fast stable branch can be observed in experiments and thus discussed in the following. In the stable branch, the spherical flame propagation speed decreases/increases monotonically with the flame radius for small/large fuel Lewis number. This is caused by the coupling between the continuously decreasing positive stretch rate and preferential thermal-fuel-mass diffusion (i.e., fuel Lewis number, Le_F) (Chen and Ju, 2007).

As shown in Figure 2, the radiative loss strongly affects the spherical flame propagation. For $Le_F = 0.5$, the spherical flame can successfully propagate outwardly until it evolves into a planar flame at $h = 0$, 0.005, and 0.01. With the increase of the radiative loss intensity, $h = 0.02$ and 0.03, the so-called self-extinguishing flame (SEF) (Ronney, 1985) is observed, and the spherical flame exists only when the flame radius is below a critical value (denoted by open circles in Figure 2a). The appearance of SEF is caused by the competition between the continuously decreasing stretch effect (which enhances the flame propagation for $Le_F < 1$) and radiative loss (Chen et al., 2010; Ronney and Sivashinsky, 1989). Different from Figure 2a, Figure 2b shows that for $Le_F = 2.0$, the spherical flame exists only when the flame radius is above a critical value (denoted by open circles in Figure 2b) for $h \geq 0.01$. This is because for large fuel Lewis number, both the positive stretch and radiative loss weaken the spherical flame propagation, and the flame cannot survive at high stretch rate (corresponding to small flame radius). As expected, the critical flame radius is shown to increase with the radiative loss. These observations are consistent with results reported in previous studies considering one-step chemistry (Chen et al., 2010; Chen and Ju, 2007; Frankel and Sivashinsky, 1983, 1984).

The peak radical concentration is known to be a good indicator of the chemical activity in premixed combustion (Glassman, 1996; Law, 2006). In Figure 3, the change of the peak radical mass fraction, Y_{Zf}, with the flame propagation speed, U, is presented. It is seen that U increases monotonically with Y_{Zf}, which is consistent with the observation based on numerical simulations by Yamamoto et al. (2009). For $Le_F = 2.0$, Figure 3b shows that U changes almost linearly with Y_{Zf}. Regarding the radiation influence, Y_{Zf} is shown to increase with h at the same U for $Le_F = 0.5$.

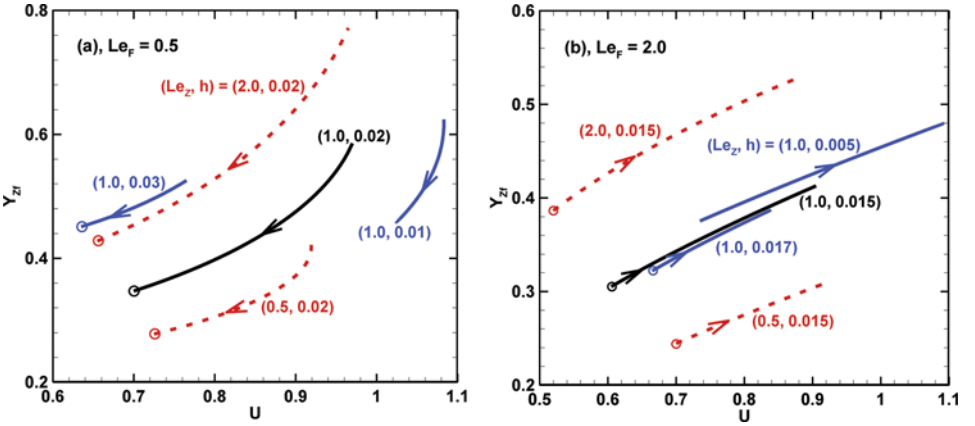

Figure 3 Change of the radical mass fraction at the flame front with flame propagation speed. The arrows indicate the direction of spherical flame propagation. The open circles correspond to solutions at the maximum (for $Le_F = 0.5$) and minimum (for $Le_F = 2.0$) flame radii shown in Figure 2. (Figure is provided in color online.)

This is because to achieve the same propagation speed, the higher the radiation intensity, the smaller the spherical flame radius (see Figure 2a) and thus the larger the flame stretch rate. The positive stretch–induced flame enhancement for $Le_F = 0.5$ 0.5 dominates over the radiative loss effect, which makes Y_{Zf} increase with h at the same U. However, for $Le_F = 2.0$, Figure 3b shows that the Y_{Zf}–U curve moves to the low-right side when the radiation intensity increases and that Y_{Zf} decreases with h at the same U.

In the above discussions, the radical Lewis number is fixed to be unity ($Le_Z = 1.0$). The influences of radical Lewis numbers on radiative spherical flame propagation are demonstrated in Figure 4. For $Le_F = 0.5$ and $Le_Z = 2.0$ in Figure 4a, the spherical flame can successfully propagate outwardly until it evolves

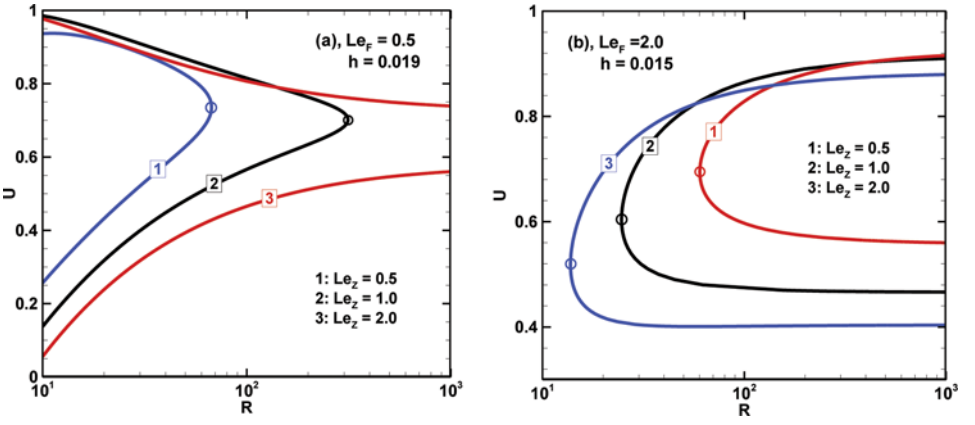

Figure 4 Spherical flame propagation at different radical Lewis numbers. (Figure is provided in color online.)

into a planar flame. However, the flame propagation trajectory changes greatly with the decrease of the radical Lewis number, and the SEF is observed for $Le_Z = 1.0$ and 0.5. For $Le_F = 2.0$, Figure 4b indicates that the critical flame radius (denoted by the open circles, below which no propagating spherical flame exists) decreases with the radical Lewis number and thus the spherical flame can survive at smaller flame radius (higher stretch rate) for mixtures with larger radical Lewis number. Therefore, according to Figures 4a and 4b, the spherical flame propagation is always enhanced by the increase of the radical Lewis number. This is due to the fact that for a positively stretched spherical flame, enthalpy loss will be caused by the radical diffusion out of the reaction zone. The larger the radical Lewis number (i.e., the smaller the radical mass diffusivity), the less the amount of enthalpy loss, and thus the stronger the flame propagation.

The influence of radical Lewis number on the Y_{Zf}–U curve is also shown in Figure 3 (see the dash-dotted lines). With the increase of Le_Z, the Y_{Zf}–U curve is shown to move upwardly, indicating that the peak radical concentration increases with the radical Lewis number. This is reasonable, since a larger amount of radicals will be accumulated at the flame front when the radical Lewis number (radical mass diffusivity) becomes larger (smaller).

The correlation between the flame propagation speed and peak radical concentration will be useful when the radical concentration in practical combustion processes can be measured through laser diagnostics. The results shown in Figure 3 from the present asymptotic analysis provide a theoretical validation to the following argument: the concentrations of some key radicals (e.g., OH or H) are indicative of laminar flame velocity or local burning velocity in premixed combustion process, which was also observed in numerical simulations (Yamamoto et al., 2009). As a result, the local burning velocity in premixed turbulent combustion in engines or combustors can be estimated based on the OH concentration, which can be measured by OH-PLIF.

Stretch Rate and Markstein Length

The outwardly propagating spherical flame is widely used to measure the unstretched laminar flame speed and Markstein length due to its well-defined stretch rate

$$K = \frac{1}{A}\frac{dA}{dt} = \frac{2}{R}\frac{dR}{dt} = \frac{2U}{R} \tag{16}$$

where $A = 4\pi R^2$ is the surface area of the spherical flame. Figures 5 and 6 show the change of the flame propagation speed with the stretch rate. The effects of radiation on the change of U with K at $Le_Z = 1$ are demonstrated in Figure 5. Consistent with theory based on one-step chemistry (Bechtold et al., 2005; Chen et al., 2010), at each radiative loss intensity, the flame propagation speed is shown to increase (decrease) with the stretch rate for $Le_F = 0.5$ ($Le_F = 2.0$). It is also seen that with the increase of the radiative loss intensity, the flame propagation is reduced and the magnitude of the gradient, $|\mathrm{d}U/\mathrm{d}K|$, increases. Therefore, the flame propagation becomes more sensitive to the stretch rate at stronger radiative loss. Moreover, the linear region

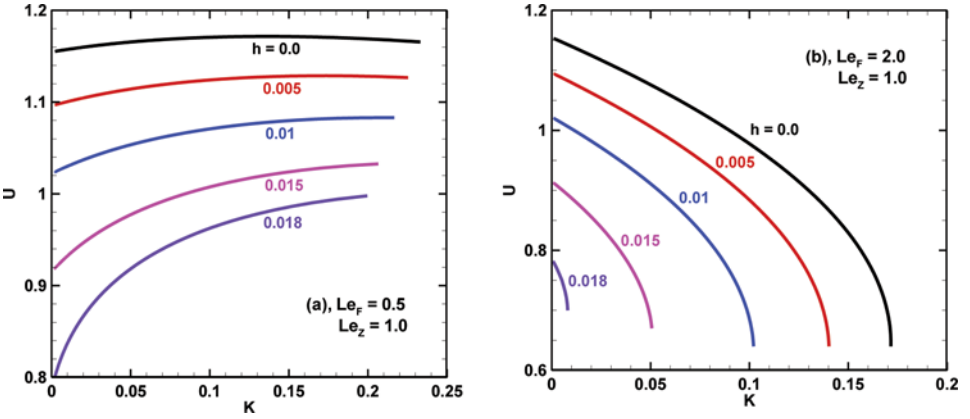

Figure 5 The flame propagation speed as a function of flame stretch at different heat loss intensities. (Figure is provided in color online.)

for U–K becomes narrower for larger radiation intensity, and very strong nonlinear behavior is observed for $h = 0.018$.

The effects of radical Lewis numbers on the change of U with K at $h = 0.01$ are shown in Figure 6. For $Le_F = 0.5$ in Figure 6a, at small stretch rate ($K < 0.02$), the linear change of U with K is observed. However, at large stretch rate ($K \geq 0.02$), U changes nonlinearly with K, and the relationship between U and K is strongly affected by the radical Lewis number. Therefore, the radical Lewis number effects become important at high stretch rate. For $Le_F = 2.0$, Figure 6b shows that the magnitude of the gradient, $|dU/dK|$, decreases with the radical Lewis number, indicating that the flame propagation becomes less sensitive to the stretch rate for mixtures with larger radical Lewis numbers.

To quantitatively assess the variation in the local flame speed due to the influence of stretching, the Markstein length needs to be introduced. At weak stretch rate,

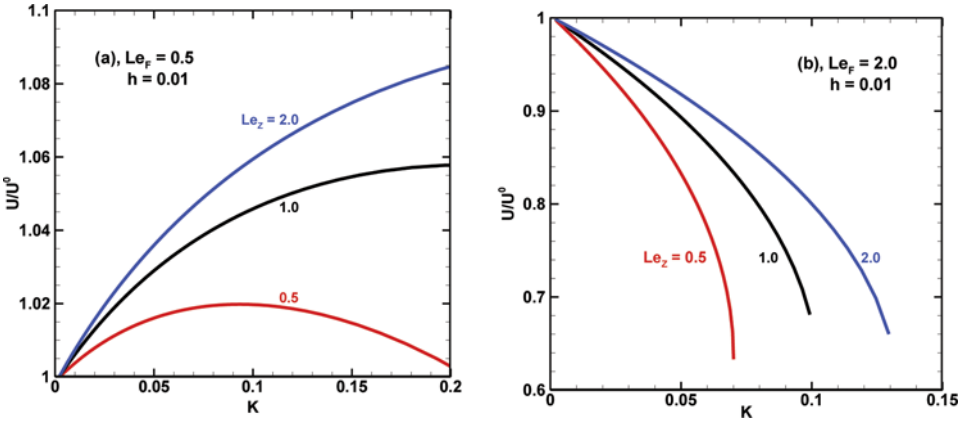

Figure 6 The normalized flame propagation speed as a function of flame stretch rate at different radical Lewis numbers. (Figure is provided in color online.)

there is a linear relationship between the flame propagation speed and stretch rate (Clavin, 1985):

$$U \approx U^0 - L \cdot K \tag{17}$$

in which U^0 is the flame speed at zero stretch rate and L is the Markstein length. It is noted that the linear relationship holds only for small stretch rate, and that U changes nonlinearly with K at large stretch rate (see Figures 5 and 6). Therefore, the Markstein length can be obtained through the linear extrapolation between U and K only for K close to zero. For adiabatic spherical flame propagation ($h = 0$), the Markstein length is found to increase/decrease monotonically with the fuel/radical Lewis number (Zhang and Chen, 2011). The opposite trends (at which the Markstein length changes with the fuel and radical Lewis numbers) are due to the fact that the radical diffuses out of the reaction zone while the fuel diffuses into it (Zhang and Chen, 2011).

Figure 7a shows the dependence of the Markstein length on fuel Lewis number at $Le_Z = 1$. It is seen that the Markstein length increases monotonically with the fuel Lewis numbers for both adiabatic ($h = 0$) and radiative ($h = 0.01$) cases. The Markstein length is shown to be influenced quantitatively but not qualitatively by the inclusion of the radiative loss. In Figure 7b, the Markstein length is shown to decrease monotonically with the radical Lewis number. These results are consistent with those shown in Figure 6. Therefore, the radiative loss does not qualitatively affect the dependence of the Markstein length on the fuel and radical Lewis numbers. Furthermore, Figure 7b indicates that the influence of radiative loss on Markstein length becomes stronger for $Le_F = 0.5$ and $Le_F = 2.0$ than that for $Le_F = 1.0$. Figure 7c presents the Markstein length as a function of radiative loss for different fuel and radical Lewis numbers. It is seen that for small radiative loss, the Markstein length is close to that of the adiabatic flame. However, when the radiative loss is large, the Markstein length is strongly affected, especially when the radiation intensity is close to that corresponding to the extinction limit discussed later. Similar observation was also found in theoretical analysis based on one-step chemistry (Matalon and Bechtold, 2009). Furthermore, as can be observed from Figure 7c, the change of the Markstein length due to radiative loss is also strongly affected by fuel and radical Lewis numbers: the change of Markstein length by radiation for ($Le_F = 1.0$, $Le_Z = 1.0$) and ($Le_F = 1.0$, $Le_Z = 2.0$) is shown to be much smaller than other cases. Moreover, only for ($Le_F = 1.0$, $Le_Z = 2.0$) does the magnitude of the Markstein length, $|L|$, decrease with the radiation intensity, h. Therefore, the sensitivity of flame propagation speed to stretch rate depends on the fuel and radical Lewis numbers as well as the radiative loss.

It should be emphasized again that the Markstein length characterizes the linear variation in the local flame speed due to the influence of external stretching only when the stretch rate is small. Because of the nonlinear change of U with K, the gradient, $-\mathrm{d}U/\mathrm{d}K$, is also a function of stretch rate (see Figures 5 and 6). Therefore, in flamelet modeling of turbulent combustion process with radiative loss, the Markstein length cannot be used to evaluate the flame speed at large stretch rate according to the linear relationship given by Eq. (17).

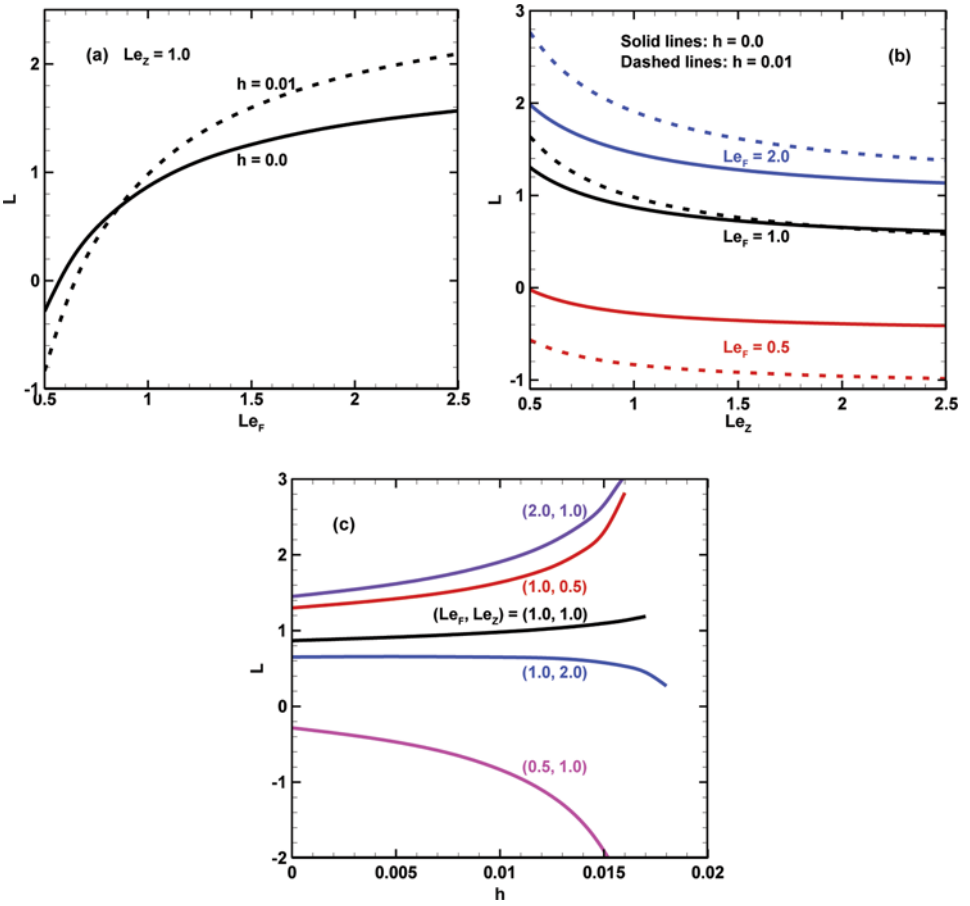

Figure 7 Effects of the fuel and radical Lewis numbers and radiative loss on the Markstein length. (Figure is provided in color online.)

Furthermore, the results shown in Figures 5 and 6 are instructive for measuring the unstretched laminar flame speed U^0 and Markstein length L using the outwardly propagating spherical flame method (Chen, 2011). As shown in Figures 5 and 6, the stretched flame speed, U, changes nonlinearly with the stretch rate, K, with the increase of radiation intensity. Therefore, for highly radiative pre-mixtures, the linear relationship between U and K given by Eq. (17) cannot be utilized to extrapolate the unstretched laminar flame speed U^0 and the Markstein length L. Besides the radiation intensity, the small radical Lewis number also results in strong nonlinear change of U with K, as shown in Figure 6. In practical experiments of outwardly propagating spherical flames, the radical Lewis number is usually less than unity while the radiation intensity depends on the equivalence ratio. For mixtures close to the lean or rich flammability limits, the radiation intensity is large, and hence the stretched flame speed changes nonlinearly with the stretch rate. Consequently, the linear relationship between U and K given by Eq. (17) cannot be utilized to

extrapolate the unstretched laminar flame speed U^0 and the Markstein length L. A nonlinear relationship between U and K should be proposed for these circumstances, which could be a topic for future study.

Extinction Limits

As shown in Figures 2 and 4, with the increase of radiation intensity, the spherical flame propagation exists only when the flame radius is below or above a critical value. Figure 8 shows the flame propagation speed as a function of radiation intensity at fixed flame radius, $R = 100$. At each value of radiation intensity, there are two flame speed solutions: the fast stable one and the slow unstable one. With the increase of radiation intensity, the difference between these two solutions becomes smaller and extinction occurs at the turning point (denoted by solid circles in Figure 8). The extinction radiation intensity at the turning point is denoted by h_c, and the spherical flame propagation occurs only for $h < h_c$. The effects of fuel Lewis number on the spherical flame extinction at $R = 100$ are demonstrated in Figure 8a. It is seen that the flammable region is extended with the decrease of fuel Lewis number. This is because at small fuel Lewis number (say, $Le_F = 0.5$), the Markstein length becomes negative. Consequently, the flame propagation is enhanced by the positive stretch rate according to Eq. (17) and is more difficult to extinguish. The same conclusion is drawn from theoretical analysis based on one-step chemistry (Bechtold et al., 2005; Chen et al., 2010).

Figure 8b demonstrates the effects of radical Lewis number on spherical flame extinction at $R = 100$. The flammable region is shown to be extended with the increase of the radical Lewis number. Again this can be explained with the help of the Markstein length, which decreases with the radical Lewis number (shown in Figure 7b). At a smaller Markstein length, the flame propagation becomes stronger at the same stretch/curvature according to Eq. (17) and thus is more difficult to extinguish. The effects of fuel and radical Lewis numbers on the extinction radiation

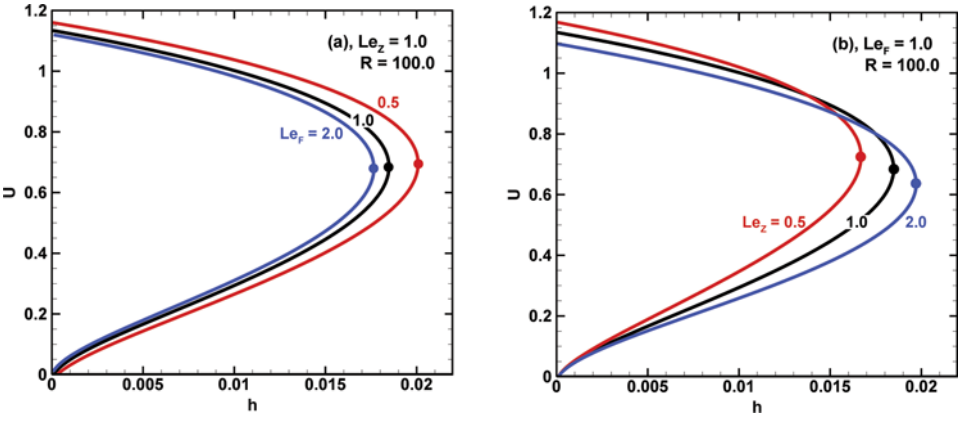

Figure 8 Change of the flame propagation speed with heat loss intensity. The solid circles denote extinction limits. (Figure is provided in color online.)

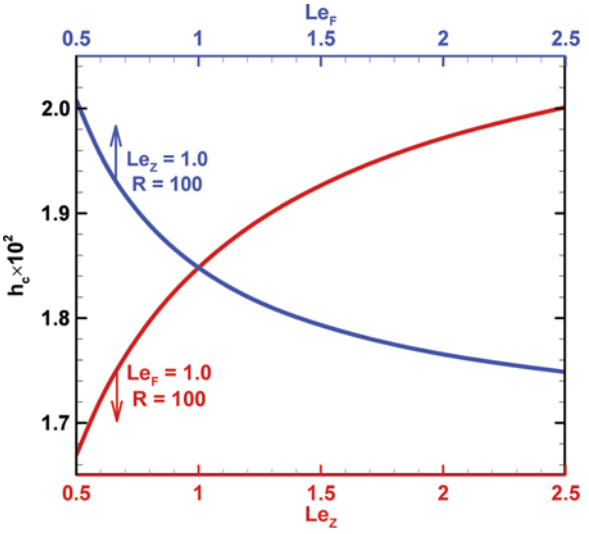

Figure 9 Change of the extinction heat loss intensity with the fuel and radical Lewis numbers. (Figure is provided in color online.)

intensity are summarized in Figure 9. As expected, the extinction radiation intensity decreases/increases monotonically with the fuel/radical Lewis number. Therefore, the flammable region of positively stretched spherical flame can be extended by decreasing the fuel Lewis number or increasing the radical Lewis number.

In the analysis mentioned above, the flame curvature is fixed ($R = 100$). Figure 10 shows the effects of flame curvature [which is inversely proportional to

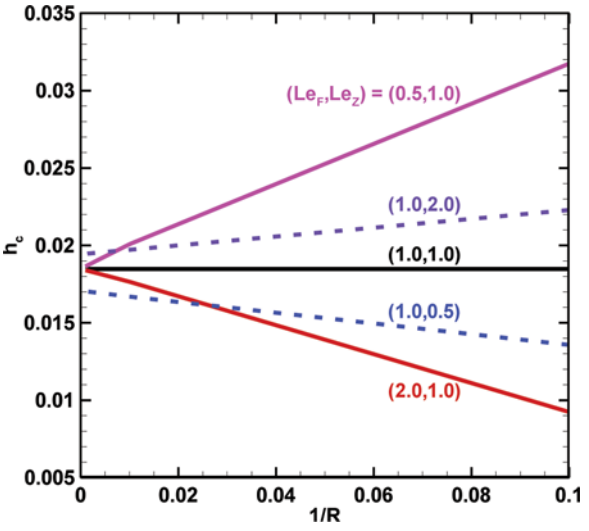

Figure 10 Change of the extinction heat loss intensity with the inverse of flame radius. (Figure is provided in color online.)

the stretch rate according to Eq. (16)] on the extinction of propagating spherical flame at different fuel and radical Lewis numbers. At the same radical Lewis number, $Le_Z = 1.0$, the extinction radiation intensity, h_c, is shown to increase and decrease monotonically with the inverse of flame radius, R^{-1}, for $Le_F = 0.5$ and $Le_F = 2.0$, respectively. However, at the same fuel Lewis number, $Le_F = 1.0$, h_c is shown to monotonically decrease and increase with R^{-1} for $Le_Z = 0.5$ and $Le_Z = 2.0$, respectively. The opposite effects of fuel and radical Lewis number are due to the fact that the fuel and radical diffuse in the opposite directions. Moreover, the radiative spherical flame propagation exists only at small flame radius when h_c increases with R^{-1}. Therefore, according to Figure 10, the SEF can be observed for mixtures with small fuel Lewis number and/or large radical Lewis number (for which $\partial h_c/\partial R^{-1} > 0$).

It is noted that flame extinction caused by radiation is one of the important problems in ultralean combustion utilized in high-efficiency low-emission engines. The flame extinction could be a source of unburned hydrocarbon and constitute a loss in the combustion efficiency in internal combustion engines. Moreover, excessive radiation–induced heat loss results in significant increases in the Markstein length (see Figure 7c) and thereby would lead to ignition failure (Chen et al., 2011; Chen and Ju, 2007). What is more, it is also of interest to allow for the transport effects of radical and/or intermediates (quantified as radical Lewis number) on flame extinction. In ultralean combustion, the transport characteristics of radicals strongly affect the flame reactivity and the extinguishment.

Comparison Between Linear and Quartic Heat Loss Models

In this subsection, the influences of linear ($n = 1$) and quartic ($n = 4$) heat loss models on spherical flame propagation are compared, and the results are plotted in Figure 11.

The change of the flame propagation speed with the flame radius at different heat loss intensities is shown in Figure 11a. In order to get close results from the linear and quartic heat loss models, we choose the linear heat loss intensity to be 3.5 times the quartic/radiation heat loss intensity. The results at $h = 0.01$ for $n = 4$ are shown to be nearly the same as those at $h = 0.035$ for $n = 1$. At a higher heat loss intensity, $h = 0.02$ for $n = 4$ and $h = 0.07$ for $n = 1$, quantitative agreement between the results from these two heat loss models is also observed in Figure 11a.

Figure 11b shows the dependence of the Markstein length on fuel and radical Lewis numbers in cases of linear and quartic heat loss models. Again, it is seen that the results for both models are nearly the same when the linear heat loss intensity is 3.5 times the quartic/radiation heat loss intensity. The extinction heat loss intensity as a function of fuel and radical Lewis numbers predicted by linear and nonlinear heat loss models is compared in Figure 11c, where the extinction radiative loss intensity ($n = 4$) is magnified to be 3.5 times its original value for clear comparison with the extinction linear heat loss intensity ($n = 1$). Although the quantitative discrepancy (<12%) exists between the extinction of the heat loss intensities of the linear and quartic models, qualitative agreement is still achieved.

Therefore, the linear ($n = 1$) and quartic ($n = 4$) heat loss models have qualitatively and even quantitatively similar influence on spherical flame propagation when the heat loss intensities are properly specified. Though linear heat loss (i.e., $n = 1$)

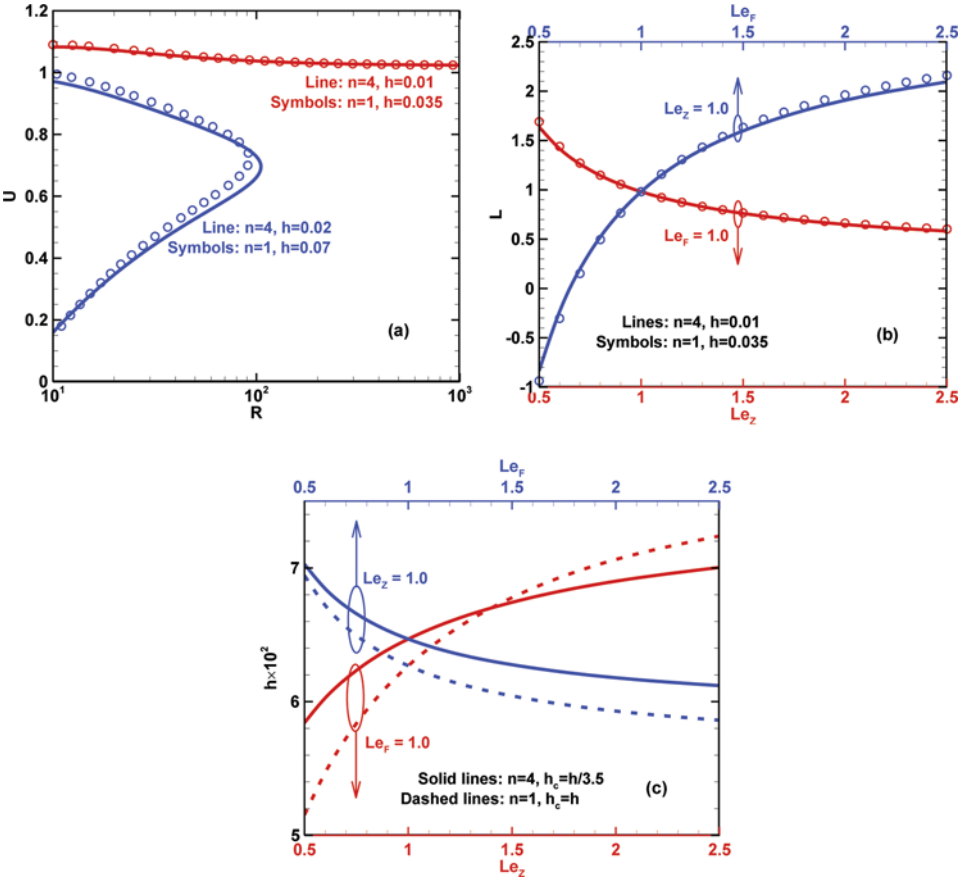

Figure 11 Comparison between linear ($n=1$) and quartic ($n=4$) heat loss models in terms of (a) spherical flame propagation speed for $Le_F=0.5$ and $Le_Z=1.0$, (b) Markstein length, and (c) extinction heat loss intensity at $R=100$. (Figure is provided in color online.)

was considered in previous studies (Chen et al., 2010; Chen and Ju, 2007; Dold, 2007; Dold et al., 2002, 2003, 2004), for the simplicity of mathematical manipulations, qualitatively correct results were obtained according to the above discussions.

In novel combustion devices such as micro- and mesoscale combustors, heat loss plays an important role, which can result in flame quenching (Ju and Maruta, 2011). In micro- and mesoscale combustors, heat loss is essentially the combined effect of volumetric radiation, convection, and heat conduction between the flame and the wall surface of the combustor. In some reported investigations on flame extinction in microscale combustors (Ju and Xu, 2005) or channels (Daou and Matalon, 2002; Nakamura et al., 2012; Xu and Ju, 2009), the linear model with respect to the temperature was utilized to mimic the heat loss, and reasonable results were obtained. According to the results presented in this subsection, it is sound to use the linear heat loss model, instead of the quartic one, to assess the influences of heat loss on flame extinguishment.

NUMERICAL VALIDATION

In the above theoretical analysis, the spherical flame propagation is assumed in a quasisteady ($\partial/\partial\tau = 0$) and quasiplanar ($R >> 1$) manner. Therefore, the unsteady transition effects and higher order terms of $O(R^{-2})$ are not included in the theoretical correlation given by Eq. (15). Moreover, the theoretical analysis is based on the large activation energy assumption, and the reaction zone is assumed to be infinitely thin. In the following, transient numerical simulations of spherical flame propagation at finite reaction rate are conducted to check the applicability of the theoretical results under more realistic conditions.

The time-dependent system given by Equation (2) is solved numerically by means of an implicit finite volume method (Chen et al., 2010). The finite reaction rate given in Eq. (3) with $\beta = 10$ and $\sigma = 0.778$ ($\gamma = 0.286$) and the radiative heat loss ($n = 4$) are considered in the numerical simulation. To numerically resolve the moving flame front, an eight-level adaptive gridding algorithm (Chen, 2010; Chen et al., 2010) is employed. The mesh addition and removal are based on the first- and second-order gradients of the temperature distribution. In all simulations, the computation domain is $0 \le r \le 1600$. The boundary conditions of zero gradient for temperature and fuel mass fraction are used at both $r = 0$ and $r = 1600$. To initialize the flame, the planar flame solution (with the flame front at $R = 2 \sim 12$) is used as the initial condition so that the outwardly propagating spherical flame can be successfully initialized.

To justify the validity of the quasisteady state assumption used in theoretical analysis, the magnitude of the unsteady term is evaluated. The numerical results from transient simulation are transformed into the flame front attaching coordinate (in which theoretical analysis is conducted). In the transformed coordinate, the magnitudes of unsteady term ($\partial T/\partial t + U\partial T/\partial r$), convection term ($-U\partial T/\partial r$), diffusion term ($\partial(\partial T/r^2\partial \mathrm{r})/r^2\partial r$), radiative loss term ($-h[(T+\gamma)^4 - \gamma^4]$), and reaction term ($\omega$) in the energy equation are compared, and the importance of the unsteady effects can be revealed by comparing the unsteady term with other terms. Figure 12 shows the results for a flame at $R = 15$. It is seen that the unsteady term is much smaller than all other terms, and thereby can be neglected in theoretical analysis. Other simulation results demonstrate that the unsteady effects are noticeable only when the flame radius is small ($R < 10 \sim 20$) and that the magnitude of the unsteady term decreases with the flame radius. Therefore it is reasonable to employ the quasisteady state assumption for $R >> 1$.

The numerical results on the spherical flame propagation speed as a function of flame radius at different radiation intensities are plotted in Figure 13. The unstable U–R branch can only be obtained in theoretical analysis and cannot be predicted by transient numerical simulation. Therefore, the numerical results in Figure 13 agree qualitatively with the theoretical results in Figure 2. The numerical results at $R = 10 \sim 20$ are affected by the initial condition (i.e., unsteady flame transition), and therefore the turning points in Figure 2b for $Le_F = 2.0$ cannot be predicted in numerical simulation. Nevertheless, the SEF is observed in the simulation for $Le_F = 0.5$ shown in Figure 13a.

The normalized flame propagation speed as a function of flame stretch rate for $Le_F = 0.5$ and $h = 0.01$ is shown in Figure 14. It is seen that U changes nonlinearly

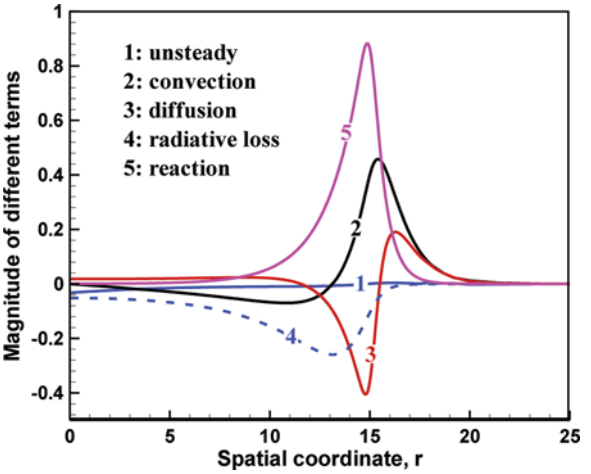

Figure 12 The unsteady term ($\partial T/\partial t + U\partial T/\partial r$), convection term ($-U\partial T/\partial r$), diffusion term ($\partial(\partial T/r^2\partial r)/r^2\partial r$), radiative loss term ($-h[(T+\gamma)^4-\gamma^4]$), and reaction term ($\omega$) of the energy equation in the the flame front attaching coordinate. $R=15$, $Le_F=0.5$, $Le_Z=1.0$, and $h=0.04$. (Figure is provided in color online.)

with K, and the radical Lewis number strongly affects the change of U with K. Again, qualitative agreement with theoretical results in Figure 6a is achieved. It is noted that at large stretch rate ($K=0.14\sim0.2$) and thus small flame radius ($R=10\sim14$), the results are affected by the initial condition in the numerical simulation. Therefore, the simulation results at $K=0.14\sim0.2$ are different from those from theoretical analysis.

Figure 15 presents the Markstein length predicted by numerical simulation. Similar to the theoretical results in Figure 7c, the Markstein length is slightly influenced by radiation at low radiative intensity, while it is strongly affected when

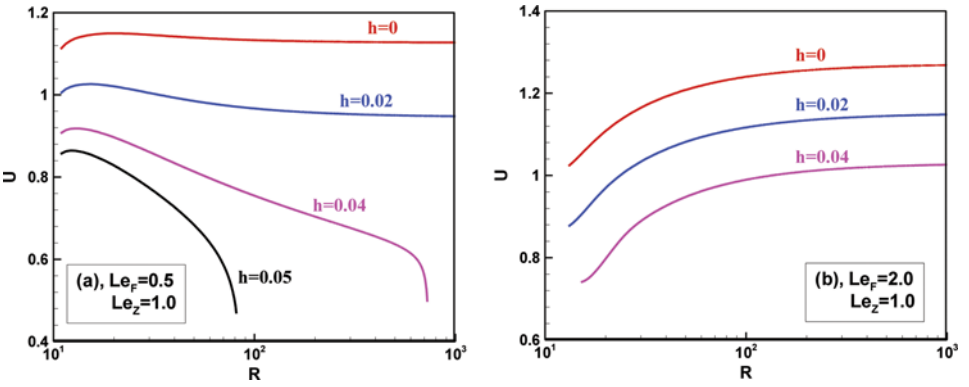

Figure 13 Change of the spherical flame propagation speed with the flame radius. (Figure is provided in color online.)

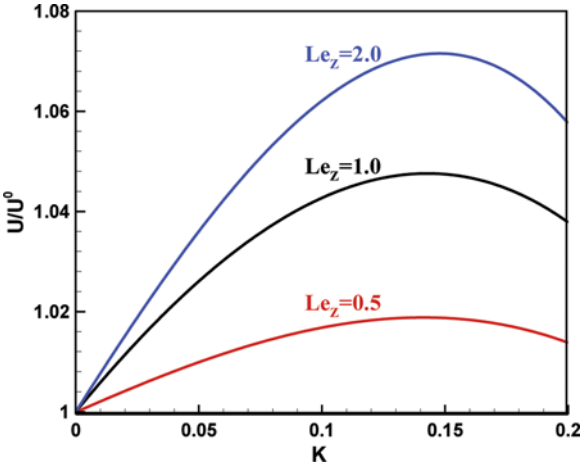

Figure 14 The normalized flame propagation speed as a function of flame stretch rate for $Le_F = 0.5$ and $h = 0.01$. (Figure is provided in color online.)

the radiative intensity is close to that corresponding to the extinction limit. Moreover, the change of the Markstein length due to radiative loss is strongly affected by fuel and radical Lewis numbers. There, observations are consistent with theoretical results in Figure 7c. Compared to the theoretical analysis, the radiation intensity at the extinction limit is shown to be much larger in simulation (see Figures 2, 7c, 13, and 15). This might be because finite activation energy ($\beta = 10$) is considered in the numerical simulation. Nevertheless, the numerical results in Figures 12–15 agree qualitatively with the theoretical results in the previous section.

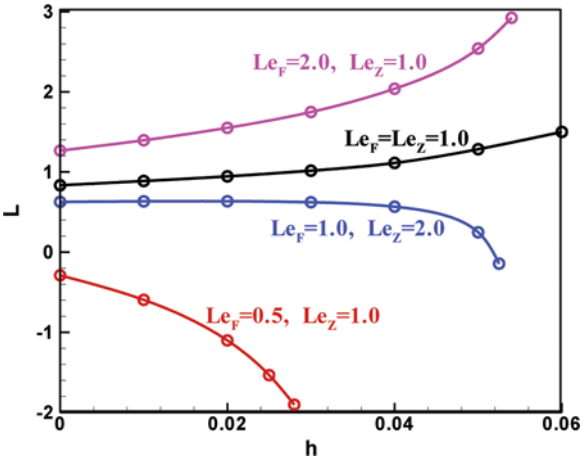

Figure 15 Change of the Markstein length with radiative loss intensity. (Figure is provided in color online.)

CONCLUSIONS

The outwardly propagating spherical flames with thermally sensitive intermediate kinetics and radiative loss are analyzed, and the correlation between the flame propagation speed and flame radius is derived based on the quasisteady and quasiplanar assumptions. With the help of this correlation, the spherical flame propagation and extinction are studied. The main conclusions are as follows:

1. The spherical flame propagation is strongly affected by fuel and radical Lewis numbers and radiative loss. The flame propagation speed correlates well with the peak radical concentration, and it is also strongly affected by fuel and radical Lewis numbers and radiative loss. The effects of fuel Lewis number and radiative loss are similar to those found in analysis based on one-step chemistry. The increase of the radical Lewis number is found to always enhance spherical flame propagation.
2. The spherical flame propagation is more sensitive to the stretch rate at stronger radiative loss and/or smaller radical Lewis number. Strong nonlinear behavior between flame propagation speed and stretch rate is observed at high radiation intensity or large stretch rate. The radiative loss does not qualitatively affect the dependence of the Markstein length on the fuel and radical Lewis numbers. However, quantitative effects of radiation do exist: For small radiative loss, the Markstein length is close to that of the adiabatic flame; when the radiative loss is large, the Markstein length is greatly affected.
3. The extinction radiation intensity decreases/increases with the fuel/radical Lewis number. Therefore, the flammable region of the positively stretched spherical flame can be extended by decreasing the fuel Lewis number or increasing the radical Lewis number. The change of the extinction radiation intensity with flame curvature/stretch is found to be strongly affected by fuel and radical Lewis numbers. It is shown that the SEF can be observed for mixtures with small fuel Lewis number and/or large radical Lewis number.
4. Both the linear and quartic heat losses can be considered in the present analysis by specifying $n = 1$ and $n = 4$, respectively. Comparison between the effects of these two types of heat loss on spherical flame propagation is conducted. The linear and quartic heat loss models are found to have qualitatively and even quantitatively similar influence on spherical flame propagation when the heat loss intensities are properly specified.

It is noted that the theory is constrained by quasisteady, quasiplanar, and large activation energy assumptions. In order to confirm the validity of the theoretical prediction, transient numerical simulations of spherical flame propagation at finite reaction rate are conducted. It is shown that the results from the theoretical analysis agree qualitatively with those from numerical simulation.

ACKNOWLEDGMENTS

This work was sponsored by the National Natural Science Foundation of China (No. 50976003 and No. 51136005) and Doctoral Fund of Ministry of

Education of China (Grant No. 20100001120003). The authors thank Professor Yiguang Ju at Princeton University for helpful discussions.

REFERENCES

Bechtold, J.K., Cui, C., and Matalon, M. 2005. The role of radiative losses in self-extinguishing and self-wrinkling flames. *Proc. Combust. Inst.*, **30**, 177–184.

Bechtold, J.K., and Matalon, M. 1987. Hydrodynamic and diffusion effects on the stability of spherically expanding flames. *Combust. Flame*, **67**(1), 77–90.

Buckmaster, J., and Lee, C.J. 1992. The effects of confinement and heat loss on outwardly propagating spherical flames. *Proc. Combust. Inst.*, **24**(1), 45–51.

Champion, M., Deshaies, B., Joulin, G., and Kinoshita, K. 1986. Spherical flame initiation - theory versus experiments for lean propane-air mixtures. *Combust. Flame*, **65**(3), 319–337.

Chen, Z. 2010. Effects of radiation and compression on propagating spherical flames of methane/air mixtures near the lean flammability limit. *Combust. Flame*, **157**, 2267–2276.

Chen, Z. 2011. On the extraction of laminar flame speed and Markstein length from outwardly propagating spherical flames. *Combust. Flame*, **158**, 291–300.

Chen, Z., Burke, M.P., and Ju, Y. 2011. On the critical flame radius and minimum ignition energy for spherical flame initiation. *Proc. Combust. Inst.*, **33**, 1219–1226.

Chen, Z., Gou, X., and Ju, Y. 2010. Studies on the outwardly and inwardly propagating spherical flames with radiative loss. *Combust. Sci. Technol.*, **182**, 124–142.

Chen, Z., and Ju, Y. 2007. Theoretical analysis of the evolution from ignition kernel to flame ball and planar flame. *Combust. Theor. Model.*, **11**(3), 427–453.

Chen, Z., and Ju, Y. 2008. Combined effects of curvature, radiation, and stretch on the extinction of premixed tubular flames. *Int. J. Heat Mass Transfer*, **51**, 6118–6125.

Chen, Z., Qin, X., Xu, B., Ju, Y.G., and Liu, F.S. 2007. Studies of radiation absorption on flame speed and flammability limit of CO_2 diluted methane flames at elevated pressures. *Proc. Combust. Inst.*, **31**, 2693–2700.

Chung, S.H., and Law, C.K. 1988. An integral analysis of the structure and propagation of stretched premixed flames. *Combust. Flame*, **72**(3), 325–336.

Clavin, P. 1985. Dynamic behavior of premixed flame fronts in laminar and turbulent flows. *Prog. Energy Combust. Sci.*, **11**(1), 1–59.

Daou, J., and Matalon, M. 2002. Influence of conductive heat-losses on the propagation of premixed flames in channels. *Combust. Flame*, **128**(4), 321–339.

Dold, J.W. 2007. Premixed flames modelled with thermally sensitive intermediate branching kinetics. *Combust. Theor. Model.*, **11**(6), 909–948.

Dold, J.W., Thatcher, R.W., Omon-Arancibia, A., and Redman, J. 2002. From one-step to chain-branching premixed flame asymptotics. *Proc. Combust. Inst.*, **29**(2), 1519–1526.

Dold, J.W., Weber, R.O., and Daou, J. 2004. Reactive-diffusion stability of premixed flames with modified Zel'dovich-Liñán kinetics. In Higuera, F.J., Jimenez, J., and Vega, J.M. (Eds.), *Simplicity, Rigor and Relevance in Fluid Mechanics*, CIMNE, Barcelona, Spain.

Dold, J.W., Weber, R.O., Thatcher, R.W., and Shah, A.A. 2003. Flame balls with thermally sensitive intermediate kinetics. *Combust. Theor. Model.*, **7**(1), 175–203.

Frankel, M.L., and Sivashinsky, G.I. 1983. On effects due to thermal-expansion and Lewis number in spherical flame propagation. *Combust. Sci. Technol.*, **31**(3–4), 131–138.

Frankel, M.L., and Sivashinsky, G.I. 1984. On quenching of curved flames. *Combust. Sci. Technol.*, **40**, 257–268.

Glassman, I. 1996. *Combustion*. Academic Press, San Diego, CA.

Gubernov, V.V., Kolobov, A.V., Polezhaev, A.A., and Sidhu, H.S. 2011. Oscillatory thermal-diffusive instability of combustion waves in a model with chain-branching reaction and heat loss. *Combust. Theor. Model.*, **15**(3), 385–407.

Gubernov, V.V., Sidhu, H.S., and Mercer, G.N. 2008a. Combustion waves in a model with chain branching reaction and their stability. *Combust. Theor. Model.*, **12**(3), 407–431.

Gubernov, V.V., Sidhu, H.S., Mercer, G.N., Kolobov, A.V., and Polezhaev, A.A. 2008b. The effect of Lewis number variation on combustion waves in a model with chain-branching reaction. *J. Math. Chem.*, **44**(3), 816–830.

He, L.T. 2000. Critical conditions for spherical flame initiation in mixtures with high Lewis numbers. *Combust. Theor. Model.*, **4**(2), 159–172.

Joulin, G., and Clavin, P. 1979. Linear-stability analysis of non-adiabatic flames—diffusional-thermal model. *Combust. Flame*, **35**(2), 139–153.

Ju, Y., Maruta, K., and Niioka, T. 2001. Combustion limits. *Appl. Mech. Rev.*, **54**, 257–277.

Ju, Y.G., and Maruta, K. 2011. Microscale combustion: Technology development and fundamental research. *Prog. Energy Combust. Sci.*, **37**(6), 669–715.

Ju, Y.G., and Xu, B. 2005. Theoretical and experimental studies on mesoscale flame propagation and extinction. *Proc. Combust. Inst.*, **30**, 2445–2453.

Kelley, A.P., Bechtold, J.K., and Law, C.K. 2012. Premixed flame propagation in a confining vessel with weak pressure rise. *J. Fluid Mech.*, **691**, 26–51.

Law, C.K. 2006. *Combustion Physics*. Cambridge University Press, Cambridge, UK.

Linan, A., and Williams, F.A. 1993. *Fundamental Aspect of Combustion*, Oxford University Press, New York.

Matalon, M., and Bechtold, J.K. 2009. A multi-scale approach to the propagation of non-adiabatic premixed flames. *J. Eng. Math.*, **63**, 309–326.

Nakamura, H., Fan, A., Minaev, S., Sereshchenko, E., Fursenko, S., Tsuboi, Y., and Maruta, K. 2012. Bifurcations and negative propagation speeds of methane/air premixed flames with repetitive extinction and ignition in a heated microchannel. *Combust. Flame*, **159**(4), 1631–1643.

Ronney, P.D. 1985. Effect of gravity on laminar premixed gas combustion. 2. Ignition and extinction phenomena. *Combust. Flame*, **62**(2), 121–133.

Ronney, P.D., and Sivashinsky, G.I. 1989. A theoretical-study of propagation and extinction of nonsteady spherical flame fronts. *SIAM J. Appl. Math.*, **49**(4), 1029–1046.

Sharpe, G.J., and Falle, S.A.E.G. 2011. Numerical simulations of premixed flame cellular instability for a simple chain-branching model. *Combust. Flame*, **158**, 925–934.

Taylor, S.C. 1991. Burning velocity and the influence of flame stretch. Ph.D. thesis, University of Leeds, Leeds, UK.

Westbrook, C.K. 2000. Chemical kinetics of hydrocarbon ignition in practical combustion systems. *Proc. Combust. Inst.*, **28**(2), 1563–1577.

Xu, B., and Ju, Y.G. 2009. Studies on non-premixed flame streets in a mesoscale channel. *Proc. Combust. Inst.*, **32**, 1377–1382.

Yamamoto, K., Ozeki, M., Hayashi, N., and Yamashita, H. 2009. Burning velocity and OH concentration in premixed combustion. *Proc. Combust. Inst.*, **32**, 1227–1235.

Zeldovich, Y.B., Barenblatt, G.I., Librovich, V.B., and Makhviladze, G.M. 1985. *The Mathematical Theory of Combustion and Explosions*, Consultants Bureau, New York.

Zhang, H., and Chen, Z. 2011. Spherical flame initiation and propagation with thermally sensitive intermediate kinetics. *Combust. Flame*, **158**, 1520–1531.

Zhang, H., Guo, P., and Chen, Z. 2013. Critical condition for the ignition of reactant mixture by radical deposition. *Proc. Combust. Inst.*, **34**, 3267–3275.